

Fiber Bragg Gratings for Strain Sensing in High Temperature Superconducting Magnet

Q. Wang, Z. Fen, F. Deng, G. Huang, L. Yan, and Y. Dai

Abstract—Fiber Bragg grating (FBG) for measuring stress and strain in 77 K and high magnetic field environment for a high temperature superconducting (HTS) magnet has been studied. The sensing characteristics of FBG in the cryogenic environment were studied on the basis of a series of experiments. To study the strain sensing behavior of FBG at 77 K, the principle of the cantilever which used an aluminum plate clamped at one end and deployed as a cantilever was applied. The results demonstrated that the FBGs still possess good linear strain sensing property at liquid nitrogen temperature. The function of micro-strain and wavelength shift is determined as $\Delta\lambda_B = 1.23 \mu\epsilon_z$ at 77 K. Based on this equation, the hoop strain of a HTS magnet wounded by Bi2223 was measured. The hoop strain difference between the measured results by FBG and the calculated results by ANSYS is very small.

Index Terms—HTS coil, liquid nitrogen temperature, strain sensitivity, strain sensor.

I. INTRODUCTION

THE development of high field superconducting magnets combined with the use of advanced composite materials creates a requirement for monitoring the integrity of support structures to avoid the quench of superconducting magnet [1]. The applications of conventional strain gauge technology are severely limited by the presence of high magnetic fields and the highly non-linear temperature dependence of the response of resistive foil strain gauges [2]. The dimensions of the strain gauges and associated electrical connections also limit their applicability in compact systems. Optical Fiber Bragg gratings (FBG) have been extensively studied for structural health monitoring, with a large number of reports of application and field trials [3]. The small dimensions of the optical fiber combined with the possibility of embedment within composite structures and the multiplexing capability of FBG sensors make them an attractive proposition for this application. In addition to the measurement of stress and strain, the small magnetic field sensitivity of FBGs will be exploited to develop a multiplexed magnetic field sensor. The applicability of the FBG would not be limited to superconductors, but also to any cryogenic structure such as those used in the large particle physics experiments. The stress and strain characteristics of FBG in the high magnetic field super-

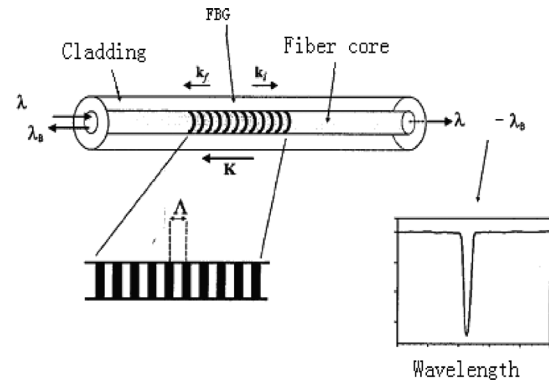


Fig. 1. Principle for fiber Bragg grating.

conducting magnet are essential to obtain expected operating current and magnetic field.

If the strain in the superconducting magnet exceeds a certain degree, the crack of epoxy-resin and degradation of critical current in the superconducting wire will occur. It leads to quench of superconducting magnet. In this paper, we develop a structural monitoring system operated at the cryogenic temperatures, in the presence of high magnetic fields and currents. The system will be based around the use of FBG sensors, and will be capable of monitoring strain. The technology will be used to perform measurements on a high field superconducting magnet based on a cantilever experiment to study FBG's strain behavior at 77 K to obtain the relationship between the wavelength shift and the micro-strain. The FBG sensor is used to study the strain characteristics of a HTS magnet at 77 K.

II. FIBER BRAGG GRATING STRAIN TESTING THEORY

A. Introduction of FBG

Fiber Bragg Grating (FBG) is a longitudinal periodic variation of the index of refraction in the core of an optical fiber. The spacing of the grating determined the wavelength of the reflected light. The working principle of the FBG is shown in Fig. 1. The Bragg reflection λ_B of an FBG is given as

$$\lambda_B = 2n_{eff}\Lambda \quad (1)$$

where n_{eff} is the refractive index of the core and Λ is the grating period. When only considering axial strain, the function that describes the relationship between the wavelength shift and axial strain is given as

$$\Delta\lambda_B = \lambda_B(1 - P_{ei})\epsilon_z \quad (2)$$

Manuscript received August 28, 2006. This work was supported by the National Natural Science Foundation of China (No. 10355001).

Q. Wang, Z. Fen, F. Deng, L. Yan and Y. Dai are with the Institute of Electrical Engineering, Chinese Academy of Sciences, Beijing, China (e-mail: qiu-liang@mail.iee.ac.cn; fpdeng@mail.iee.ac.cn).

G. Huang is with the Institute of Mechanics, CAS, Beijing 100080, China.

Color versions of one or more of the figures in this paper are available online at <http://ieeexplore.ieee.org>.

Digital Object Identifier 10.1109/TASC.2007.899078

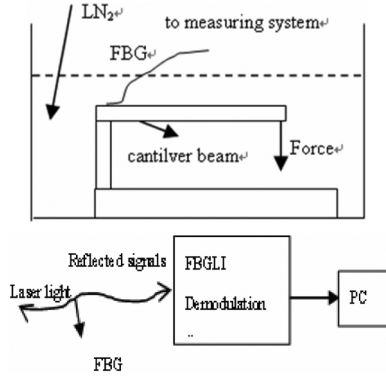


Fig. 2. Strain behavior experiment setup and FBG measuring system.

where P_{ei} is the strain sensitivity. For fused silicon fiber, the $\mu\epsilon \sim \Delta\lambda_B$ function is simplified to

$$\Delta\lambda_B = 0.78\lambda_B\epsilon_z \quad (3)$$

when the central wavelength is 1550 nm, the $\mu\epsilon \sim \Delta\lambda_B$ function is calculated as

$$\begin{aligned} \Delta\lambda_B &= 1550 \times 10^3 \times 0.78 \times 10^{-6} \mu\epsilon_z \\ &= 1.209 \mu\epsilon_z \end{aligned} \quad (4)$$

where $\mu\epsilon_z$ means the micro-strain of fiber [4]. From the (4), the micro-strain of FBG is varied linearly with the wavelength. Notice should be paid that this value is deduced at ambient temperature typically from 273 K to 300 K.

III. EXPERIMENT PROCEDURE

A. FBG Strain Behavior at 77 K

Although the characteristics of FBG strain sensors have been considerably studied, there are only a few papers dealing with their applications in the cryogenic environment. The main aim of this part was to study FBG strain sensing behavior and get its $\mu\epsilon \sim \Delta\lambda_B$ relationship at 77 K. The experiments were based on the principle of cantilever. The configuration of cantilever experiment setup is shown in Fig. 2.

The cantilever beam was made of aluminum with the rectangular cross section. One fiber Bragg grating with the Bragg wavelength of 1550 nm was mounted to one end of the beam. The strain of the FBG varied with the forces applied to the other end of the beam by loading different weights. The whole test system was immersed by liquid nitrogen (LN_2). The reflected signals from the FBG is captured by a portable demodulation system.

The FBG Bragg wavelength shift was monitored using a scanning Fabry-Perot tunable filter. The FBG demodulation, manufactured by Micron Optics, was integrated with laser source. The demodulation system had a minimum sensitivity of 1 pm and a scanning rate of 100 Hz.

The whole system including experiment setup and measuring system is showed in Fig. 2.

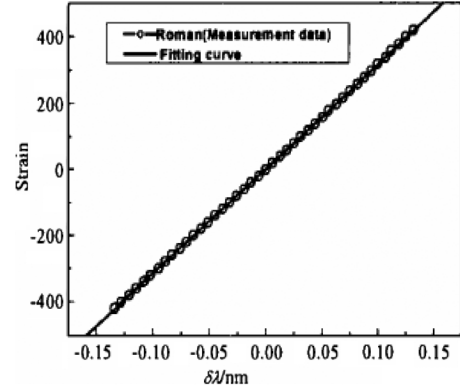


Fig. 3. Cantilever experiment result for strain vs. wavelength.

The test procedure is, first at 77 K and then at the room temperature and then at 77 K again, to investigate the behavior of FBG strain sensing in the cryogenic environment. During these tests, FBG could totally withstand the cryogenic temperature and presented a characteristic of fine flexibility and reusable ability. The strain response of the FBG was assessed at different forces applied to the cantilever beam. The forces were applied in steps of 400 g to a maximum of 2000 g.

From cantilever theory, the relationship between the applied load and the strain was given as

$$\epsilon = \frac{6gL}{Ebh^2}m \quad (5)$$

where m is the applied weight, ϵ is the strain at the end of the cantilever, g is the acceleration of gravity, E is the Young's elastic modulus of aluminum at 77 K, b and h are the wideness and the thickness of the cantilever, L is the arm of force, respectively.

It was calculated that 400 g force induces a strain of $79.8 \mu\epsilon_z$. The cantilever experimental results are illustrated in Fig. 3.

The strain changes from $-400 \mu\epsilon$ to $400 \mu\epsilon$, the positive strain values were first measured by fixing FBG on the upside of the cantilever beam, then negative strain were monitored by turning the cantilever beam upside down. The shifts of central wavelength are within the range of ± 1.5 nm. The results indicate that the strain response of the FBG is almost linear at 77 K and the slope of the $\mu\epsilon \sim \Delta\lambda_B$ curve is 1.23. Compared with theory calculated result 1.209 at the room temperature, the measured value is accurate, when material differences and system error are considered. Thus the constant 1.23 for (4) will be used in further experiments.

In order to further understand the performance of FBG strain sensor at 77 K liquid nitrogen temperature, another cantilever experiment using more advanced spectroscopy-SI720, which could monitor the whole operating spectrum, was done. During this experiment, the force was applied in steps of 200 g from 0 to a maximum of 2000 g. The spectrum of the FBG with central wavelength 1550 nm at the force of 1000 g was plotted in Fig. 4. In Fig. 4, the x -coordinate means the operating spectrum of FBG when the force applied was 1000 g, and the y -coordinate represents the reflectivity of this FBG. Carefully observation of Fig. 5 leads to an obvious result that the peak splits into

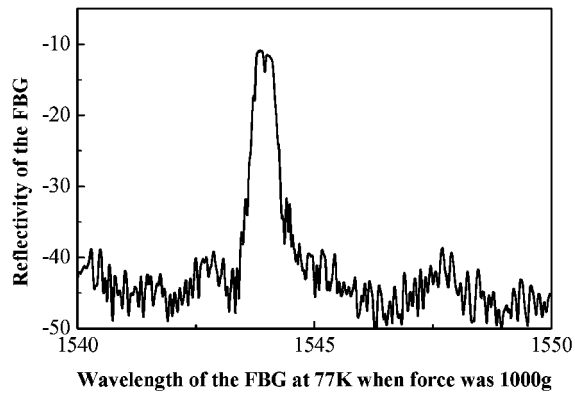


Fig. 4. Spectrum of FBG at 77 K when force was 1000 g.

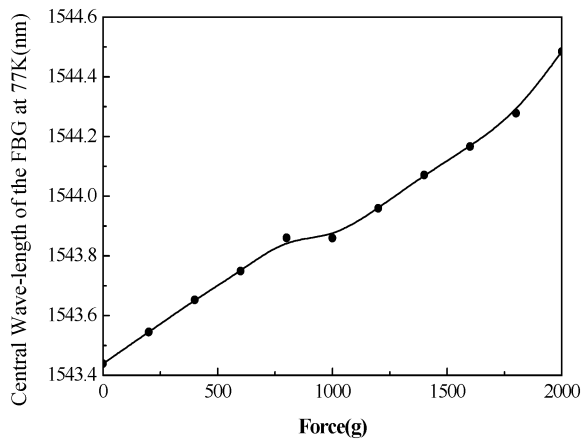


Fig. 5. Central wave-length at 77 K for FBG vs force.

two small peaks. This phenomenon was known as multi-peaks which made it hard for the demodulation system to detect and distinguish the peak of reflected lights.

Within the region of 1000 g, the FBG strain sensor had no response. This result implies that the performance of FBG strain sensor at 77 K was different from that when working at room temperature. The difference was not only in strain sensitivity of FBG at 77 K liquid nitrogen temperature, but also the strain behavior and sensing mechanism.

More effort will be endeavored to study this multi-peaks phenomenon and its influence. As this phenomenon can only be monitored with the high resolution apparatus-SLI720, we still consider that the results monitored by FBG is reliable and we will use the measured strain sensitivity by FBG during further experiments.

B. Strain Sensing in a HTS Magnet

The task of this part was to explore the feasibility of applying FBG strain sensors to monitor strain in a high temperature superconducting magnet. The experiment setup was shown in Fig. 6. The FBG sensor was stuck on the flank of the magnet. When the operating current of the magnet was below 20 A, the strain is too small to be measured, so the zero point of the strain was set to be that when the current was 20 A.

As the FBG grating has a certain length which is normally about 2 cm, the sensor actually senses both radial and hoop



Fig. 6. Experiment setup by FBG for high temperature superconducting coil.

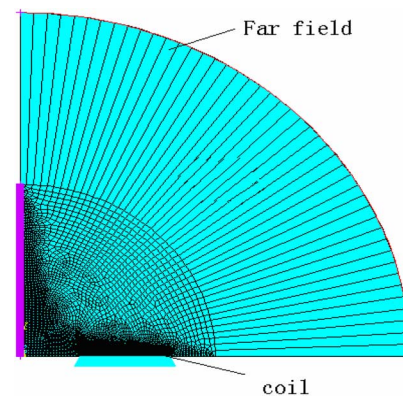


Fig. 7. Two-dimensional FEM Model for HTS magnet stress analysis.

strain produced by the magnet. However, the hoop strain is much larger than the radial strain [5], [6], the initial experiment result ignores the influence of radial strain and takes into account the hoop strain only.

C. Numerical Simulation

The finite elements method (FEM) is used to simulate the magnet strain. The finite element model of the high temperature superconducting magnet is plotted in Fig. 7.

Because the magnet is axisymmetric and the magnetic forces were assumed to be uniformly distributed in the magnet. The 2D 1/4th model was used and was treated as an isotropy solid with no need to model individual turns.

A part of the detail FEM model of the coil is plotted in Fig. 8. The high temperature superconducting magnet was wound by high temperature superconducting strip materials, Bi2223, and was impregnated with epoxy-resin. The dimension of the magnet is listed in Table I.

The mechanical properties used for simulation by ANSYS are listed in Table II. The magnet was energized by a current source. The operating current increased from 20 A all the way up to 50 A at a rate of 0.5 A/s.

D. Result Analysis

The experiment and the simulation results are illustrated in Fig. 9. From magnetic field theory, the hoop strain caused by Lorentz force is proportional to the square of operating current.

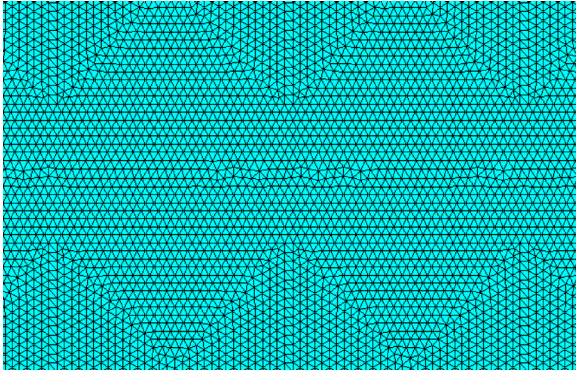


Fig. 8. A part of the detail FEM model of the coil.

TABLE I
PARAMETERS OF SUPERCONDUCTOR

Superconductor	Bi2223/AgMg
Diameter (Inner radius)	40mm
Diameter (Outer radius)	103mm
Thickness	9mm
Turns	222

TABLE II
MECHANICAL PROPERTIES OF SUPERCONDUCTOR

Mechanical Properties	Young's Elastic Modulus (MPa)	Poisson's Ratio
Superconducting Materials	600	0.28
Epoxy-Resin	3250-3805	1/3

The difference between the experimental and numerical analysis results is very small.

IV. CONCLUSIONS

The response of the FBG sensors to strain, at the cryogenic temperatures and high magnetic field is carried out in detailed. The strain sensitivity characteristics have been studied by using FBG sensor testing equipment. Based upon the results, the test system with FBG is designed with the appropriate measurement range, resolution, electrical bandwidth and sensor configuration.

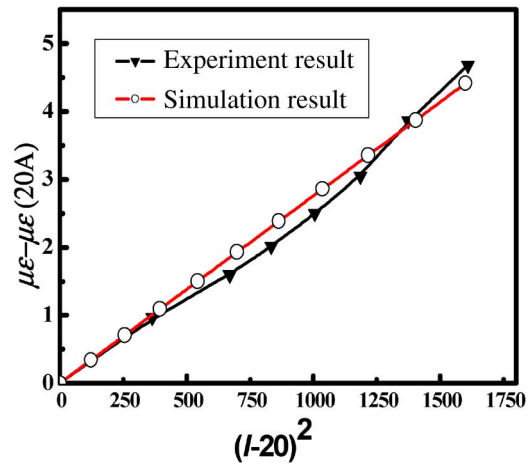


Fig. 9. Experiment result vs. simulation result.

A high temperature superconducting magnet was designed to incorporate a multiplexed array of FBG sensors, which will monitor the strains on the superconducting magnet during its operation. FBG strain sensitivity at 77 K is measured. The experimental value is close to the theoretical analysis. Then a new technology using FBG strain sensor to monitor strain in a HTS high magnetic superconducting magnet is developed.

Further experiments will study the function between the stress, strain and the central wavelength shift in the FBG under the environment of 4 K liquid helium and 20 T high magnetic field.

REFERENCES

- [1] Q. Wang, "Study of the composite winding mechanical properties by experiment and numerical simulation," *Chinese Journal of Low Temperature Physics*, vol. 25, pp. 63–70, Feb. 2003.
- [2] S. W. James and R. P. Tatam, "Strain response of fiber Bragg grating sensors at cryogenic temperature," *Measure Science and Technology*, vol. 13, pp. 1535–1539, 2002.
- [3] Y. J. Rao, "Recent progress in applications of in-fiber Bragg grating sensors," *Optics and Lasers in Engineering*, vol. 31, pp. 297–324, 1999.
- [4] Q. Wang, *High Magnetic Field Superconducting Magnet Sciences*. Syracuse, NY: Sciences Press, 2006.
- [5] E. A. Deviatkin, "Stresses in a long isotropic solenoid with longitudinally non-uniform external loads," *Cryogenics*, vol. 38, pp. 657–663, 1998.
- [6] A. W. Cox, G. W. Denis, Markiewicz, and I. R. Dixon, "Power series stress analysis of solenoid magnets," *IEEE Transactions on Magnetic*, vol. 32, pp. 3012–3015, July 1996.